Tuning energy transfer between chromophores. Switchable molecular photonic systems

Hurenkamp, Johannes Henricus

Chapter 4
Tuning of Energy Transfer Between Two Photoswitchable Coumarin-Dithienylcyclopentene Systems Through Structural Modification

The synthesis and characterisation of dithienylcyclopentene switches, with two different coumarin substituents, is described. Both functionalized switches show the reversible ring opening and closing reaction characteristic for dithienylcyclopentenes. However, only one shows reversible quenching of the coumarin fluorescence, which is unexpected considering the small differences in coumarin structure and electronic properties of the system. The reason for this large difference in energy transfer efficiency was investigated using several spectroscopic techniques as well as cyclic voltammetry and the results are rationalised in terms of the Förster and Dexter energy transfer mechanism.

4.1 Introduction

The demand for portable storage capacity, with storage density as high as possible, is rapidly approaching the limits of the top down approach of data storage (e.g. photolithography,[1] magnetic[2] / optical data storage[3]). To achieve even higher storage densities a bottom up approach may be more suitable.[4] The information density that could, potentially, be reached by using addressable individual molecules provides a strong incentive for this molecular approach. However, it also poses significant challenges with respect to addressability and fatigue resistance.

Over the past decades, a structurally diverse range of switchable molecular systems have been reported.[5] These molecules have at least two states that can be addressed separately and, preferably, have a read-out method, which does not influence the molecular state (i.e. non-destructive). Photochromic molecular switches (e.g. fulgides,[6] spiroindolizines,[7] spiropyrans[7] and dithienylcyclopentenes[8]) have shown considerable potential. The ability to change the absorption spectrum through a structural change, induced by an external stimulus (*e.g.*, pH,[9], redox,[10] irradiation[5] or temperature[11]), makes it possible to control optical properties in a reversible manner to provide functionality in a system. For example, the combination of efficient fluorophores (*e.g.*, laser dyes) with photochromic switches,[12] thereby having a unit with a high quantum yield of fluorescence ($\Phi_{fl} \approx 1$) for read out purposes, combined with an efficient switch to influence emission output, provides a highly promising approach (Figure 4.1). The properties of both parts can be optimised separately to get efficient quenching and good results have been obtained already by combining efficient chromophores (*i.e.* porphyrin, coumarin, and anthracene) with photochromic switches.[12]

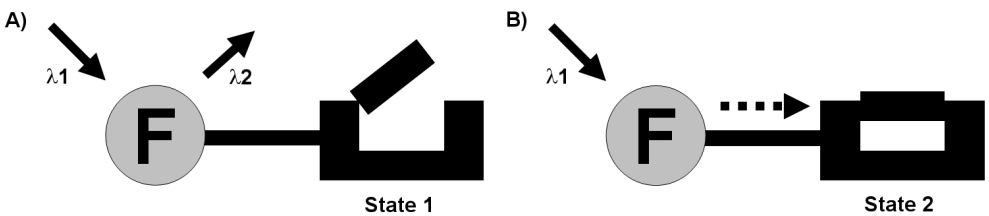

Figure 4.1 Schematic representation of a fluorophore – photochromic switch dyad. A) When the photochromic unit is in State 1, the fluorophore (F) is excited by λ1 and emits light at longer wavelengths (λ2). B) When the photochromic unit is in State 2, F is still excited by λ1, however this excited state is quenched by the photochromic unit and emission is not observed.

Dithienylcyclopentenes belong to a class of photochromic switches which show potential as photoswitchable fluorescence quenching units (Figure 4.2). The synthesis routes, which have been developed earlier, facilitate attachment of substituents (in this case chromophores). Dithienylcyclopentenes show good stability, good to very good photostationary state (PSS) and two states, with very distinct absorption spectra, which are both thermally stable.[8] Dithienylcyclopentenes already have been used successfully as switchable fluorescence quenchers, examples of which are to be found in the work of the groups of Lehn,[13] Irie,[14] Tian,[15] Branda[16] and others.[17]

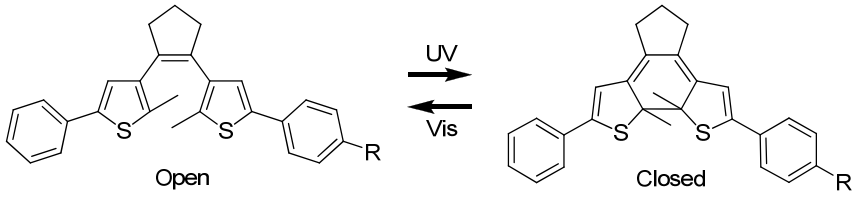

Figure 4.2 Schematic representation of the ring open and ring closed state of a dithienylcyclopentene switch.

In Chapter 3 we demonstrated that a coumarin – dithienylcyclopentene – coumarin triad system, with amide connecting units, shows up to 50% quenching of the coumarin emission in the closed (or rather PSS) state. However, this system has some disadvantages that render it unsuited for practical applications. The system shows considerable degradation at room temperature (not at 220 K) and the low PSS increases the probability of readout errors (*i.e.* when used for data storage). Adding phenyl spacers between the dithienylcyclopentene unit and the amide connecting units improves the stability considerably as well as the PSS that can be reached at room temperature.[18] Previous synthetic experience within our group has provided us with suitable starting components, both chromophores and phenyl substituted dithienylcyclopentenes,[19,20] which can be combined to build molecules that meet the requirements needed for efficient fluorescence ON/OFF switching. However, it will become clear that even if components seem to meet the basic photophysical requirements, variation in one component can hold consequences for the operation of the second component.

In this chapter two coumarin-dithienylcyclopentene systems are described, in which a minor change in the structural design of one of the components results in a considerable difference in spectroscopic properties (Figure 4.3). In the first system efficient quenching of the coumarin excited state energy in both the open and the closed state is observed. In the second system a structural change in the coumarin component, returns the high fluorescence output in the open state, which is combined with efficient quenching (>98%)

in the closed state, thereby showing the properties of a very efficient fluorescence ON / OFF switch. Both systems were investigated using a range of spectroscopic techniques (i.e. UV/Vis and fluorescence spectroscopy, cyclic voltammetry and time correlated single photon counting) to understand why such an apparently minor structural change leads to very different photophysical behaviour and to gain insight into the energy transfer processes taking place in these systems. Previously, it has been shown that ring–closing of the dithienylcyclopentene switch can be achieved by electrochemical oxidation in solution and both ring-opening and closing can be achieved when the switch is immobilised on an ITO surface.[21] Taken together this opens the possibility of electrochemical switching of fluorescence output.

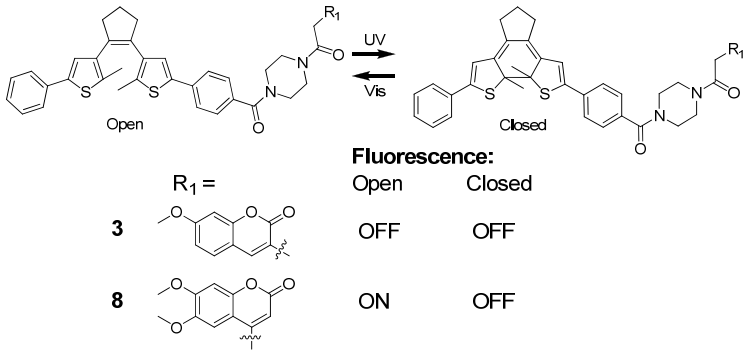

Figure 4.3 Ring-open and ring-closed state of the coumarin-dithienylcyclopentene systems (**3** and **8**) and the respective effects on the fluorescence.

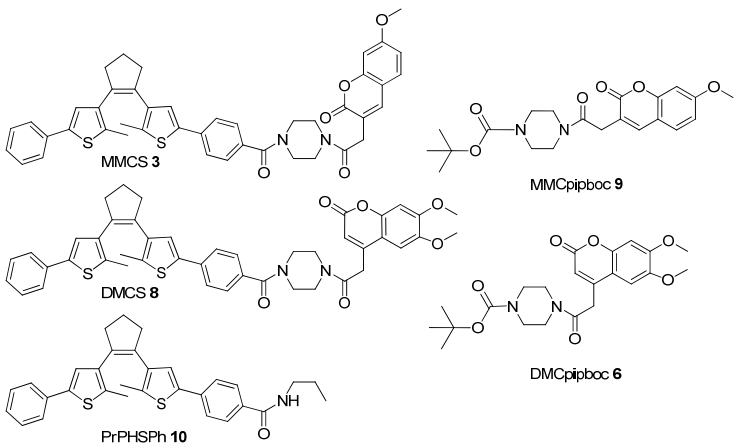

Figure 4.4 Coumarin-substituted dithienylcyclopentene switches and switch/coumarin models investigated in this chapter.

4.2 Synthesis

Amide coupling chemistry with acid functionalized dithienylcyclopentene switches has proven to be a versatile strategy in building multicomponent systems because it is a robust approach to covalent connectivity and precludes through bond intercomponent interactions.[20,22] In the synthesis of the symmetric donor-acceptor systems described in Chapters 2 and 3, amide coupling chemistry was employed successfully to connect donor fluorophores to carboxylic acid functionalized dithienylcyclopentenes and perylenes. In this chapter, the amide coupling approach is employed again to connect the coumarin donor molecules to mono acid functionalised diphenyldithienylcyclopentenes.

The carboxylic acid functionalized diphenyl switch **1** was synthesized as reported previously.[19] The synthesis of the piperazine functionalized 7-methoxy-coumarin-3-acetic acid **2** is described in Chapter 2. The mono-methoxy coumarin functionalized diphenyldithienylcyclopentene **3** was synthesized via coupling of the mono acid **1** to the 7-methoxy-coumarin-3-acetyl piperazine **2** using 2-chloro-4,6-dimethoxy-1,3,5-triazine (CDMT) and *N*-methyl-morpholine (NMM) in CH_2Cl_2, providing the monomethoxy coumarin switch (MMCS) **3** in 26% yield (Figure 4.5).[22]

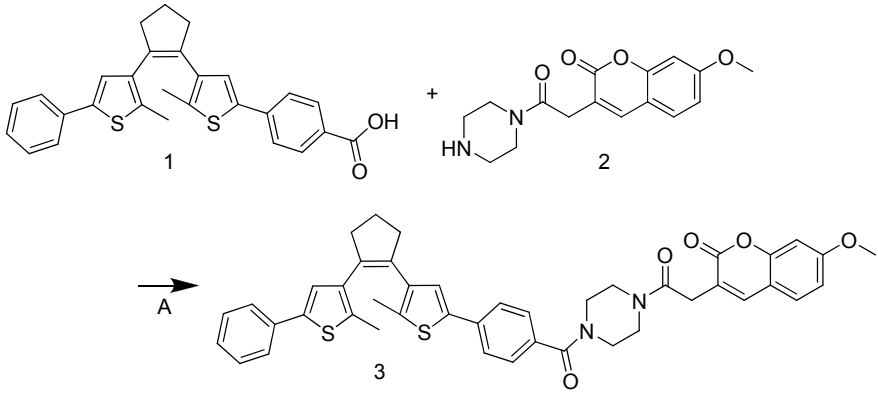

Figure 4.5 Synthesis of the mono-methoxy coumarin functionalized diphenyl switch **3** : A) i) **1** CDMT, NMM, CH_2Cl_2, 0 ^oC. ii) NMM, **2** (26%).

As will be discussed below, MMCS **3** did not meet the expectations of a fluorescence switching unit (Figure 4.3, *vide infra*). It was suspected that this was due to unfavourable energetics of the mono methoxy coumarin relative to the diphenyl switch. To solve this problem the coumarin absorption maximum needed to be shifted towards lower energy (*vide infra*: data and discussion).

A literature search revealed that a minor modification to the coumarin, *i.e.* the addition of an extra methoxy group, might have the desired effect on the coumarin absorption maximum.[23] Therefore 6,7-dimethoxy-coumarin-4-acetic acid **4** was synthesized[23] and coupled to diphenyl switch **1** using a method similar to that employed for **3**. The position of attachment for the acetic acid also changes, however, for the mono methoxy coumarin with an acetic acid on the four position spectroscopic characteristics are the same as for the mono methoxy coumarin with the attachment to the three position, so this change is expected to have little or no influence.

The 6,7-dimethoxy-coumarin-4-acetic acid **4** was coupled to *N*-Boc-piperazine **5** using 1,1'-carbonyldiimidazole (CDI). This coupling reagent facilitates purification, as was observed with the related reaction with 7-methoxy-coumarin-3-acetic acid in Chapter 2.[24] After deprotection, the piperazine functionalized dimethoxy coumarin was coupled to the mono acid diphenyl dithienylcyclopentene **1** using CDMT and NMM in CH_2Cl_2 providing the dimethoxy coumarin switch (DMCS) **8** in a moderate yield (46%, Figure 4.6).

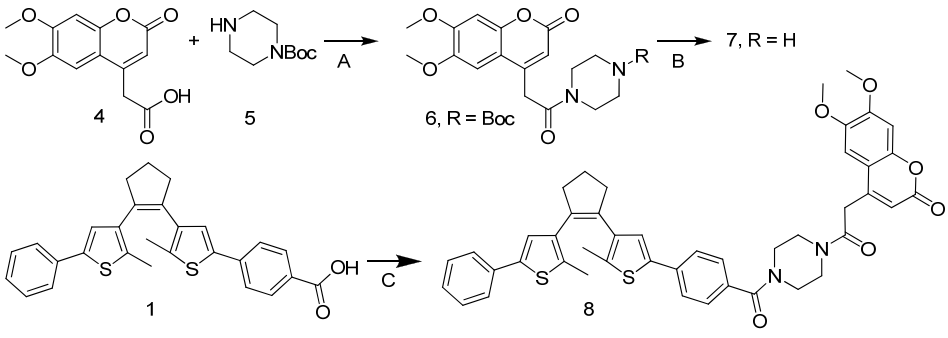

Figure 4.6 Synthesis of the di-methoxy coumarin functionalized diphenyl switch **8**: A) CDI, CH_2Cl_2, RT; B) CF_3COOH, CH_2Cl_2 ; C) i) **1**, CDMT, NMM, CH_2Cl_2, 0 ^oC. ii) NMM, **7** (46%).

All compounds were purified by column chromatography and characterized by ^1H and ^{13}C NMR spectroscopy and (MALDI-TOF) mass spectroscopy (see experimental section for details).

4.3 Electronic properties

4.3.1 Monomethoxycoumarin-dithienylcyclopentene switch 3 (MMCS)

UV/Vis spectra of MMCS **3** in the open and closed form (at the photostationary state (PSS) λ_{irr} = 365 nm) are shown in Figure 4.7. The spectra show features of both coumarin and model switch (open or $PSS_{365\ nm}$) and the maxima closely match those of the model compounds MMCpipboc **9** (*N*-Boc protected **2**) and PrPhSPh **10** (Figure 4.7 and Table 4.1), which would indicate little or no electronic communication between coumarin and dithienylcyclopentene unit.

The changes observed in the spectra of MMCS **3** and in the spectra of the model compound, PrPhSPh **10**, upon photochemical ring closure from the open state to the closed state ($PSS_{365\ nm}$) are nearly identical.[25] The similarities are more apparent by comparison of the difference spectra shown in Figure 4.8, confirming that the change seen in the absorption spectrum of **3** is due to the switching of the dithienylcyclopentene unit. The change in the absorption spectra show that the photochromism of the diphenyldithienylcyclopentene unit is retained in MMCS **3** and an excellent PSS (>95% open : closed ratio) is being achieved. Furthermore, the absorption of the coumarin moiety in **3** is unaffected by ring closure indicating that no direct electronic communication between coumarin and dithienylcyclopentene unit is present.

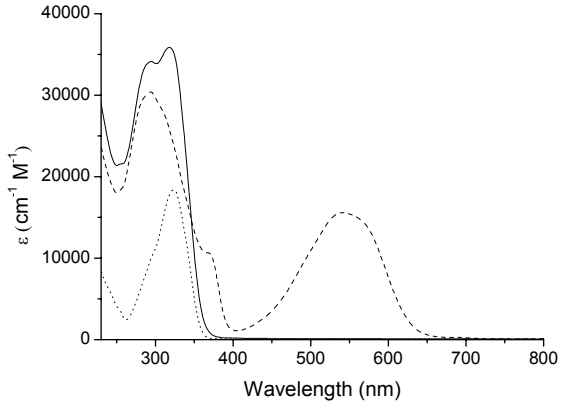

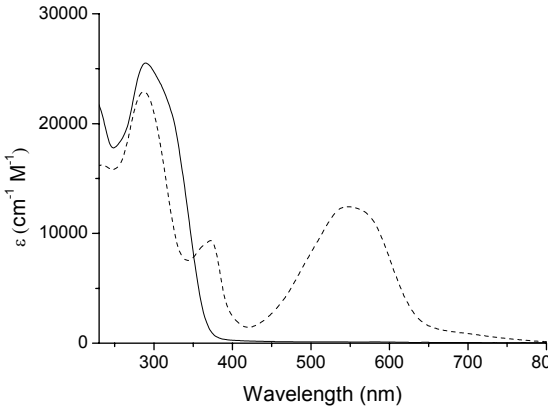

Figure 4.7 Left: UV/Vis spectra of MMCS **3** in the open state (−), $PSS_{365\ nm}$ (− − −) and MMCpipboc **9** (····), spectra recorded in CH_2Cl_2 at RT. Right: UV/Vis spectra of PrPhSPh **10** in the open state (−) and $PSS_{365\ nm}$ state (− − −), spectra recorded in CH_2Cl_2 at RT.

Table 4.1 Absorption and emission data of the dithienylcyclopentene switches in the open state and at the $PSS_{365\ nm}$ and of the appropriate model compounds.

Compound	**Absorbance[a] λ_{max} / nm (10^3 ε / cm^{-1} M^{-1})**				**Emission[a] λ_{max} / nm**
MMCpipboc **9**	-	323(18.4)	-	-	393
DMCpipboc **6**	293(4.9)	346(11.4)	-	-	417
PrPhSPh **10**	289(25.5)	-	-	-	393
PrPhSPh $PSS_{365\ nm}$ **10**[b]	287(22.9)	-	372(9.3)	547(12.4)	394
MMCS Open **3**	294(34.1)	318(35.9)	-	-	415
MMCS $PSS_{365\ nm}$ **3**[b]	294(30.4)	-	370(10.6)	541(15.6)	394
DMCS Open **8**	287(29.3)	321(24.6)	-	-	420
DMCS $PSS_{365\ nm}$ **8**[b]	285(25.9)	-	353(17.0)	541(14.9)	425

[a] Recorded in CH_2Cl_2 at RT. [b] After irradiation with λ = 365 nm light at RT till PSS was reached.

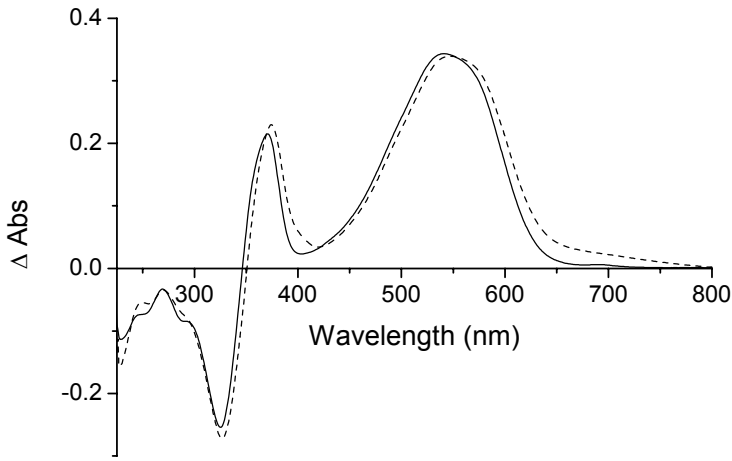

Figure 4.8 The UV/Vis difference spectra of MMCS **3** (−) and PrPhSPh **10** (− − −, normalized) obtained by subtraction of the spectrum of the open state from the spectrum of the $PSS_{365\ nm}$ state, spectra recorded in CH_2Cl_2 at RT.

Surprisingly in the open form the fluorescence of MMCS **3** is weak (< 5%) compared to that of free MMCpipboc **9**. At the $PSS_{365\ nm}$ state the position of the emission band shifts towards the blue and the intensity decreases further (Figure 4.9, left).

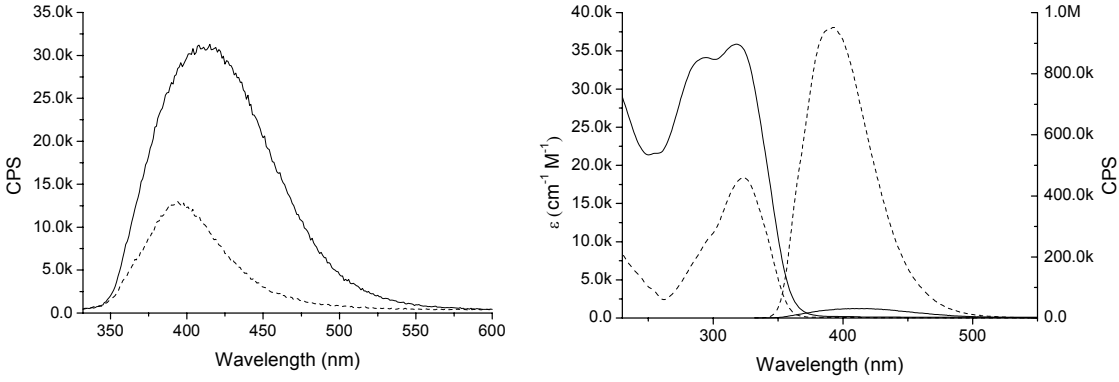

Figure 4.9 Left: Fluorescence spectra of MMCS **3** in the open state (−) and $PSS_{365\ nm}$ state (− − −), spectra recorded in CH_2Cl_2 at RT. Right: UV/Vis spectra (left side) and fluorescence spectra (right side) of MMCS **3** in the open state (−) and free MMCpipboc **9** (− − −). Fluorescence spectra were corrected for absorption at the excitation wavelength. The spectra were recorded in CH_2Cl_2 at RT.

When comparing the fluorescence intensity of the free MMCpipboc **9** with the fluorescence intensity of MMCS **3** in the open state there is almost no fluorescence visible for the open form of MMCS **3** (Figure 4.9, right). This shows that already in the open form of MMCS **3** the fluorescence of the coumarin is almost fully quenched by the dithienylcyclopentene unit, making it unsuitable for fluorescence switching (*i.e.* only OFF/OFF states are available).

4.3.2 Dimethoxycoumarin dithienylcyclopentene switch 8 (DMCS)

The UV/Vis absorption spectra of DMCS **8** in the open and closed form (at the photo stationary state ($PSS_{365\ nm}$)) are shown in Figure 4.10 left. As for MMCS **3**, the spectra show features of both the dimethoxy coumarin component and of the open or $PSS_{365\ nm}$ model switch, respectively, and the absorption maxima match those of the spectrum obtained by adding the individual spectra of model compounds 6 and 10 (Table 4.1, Figure 4.23).

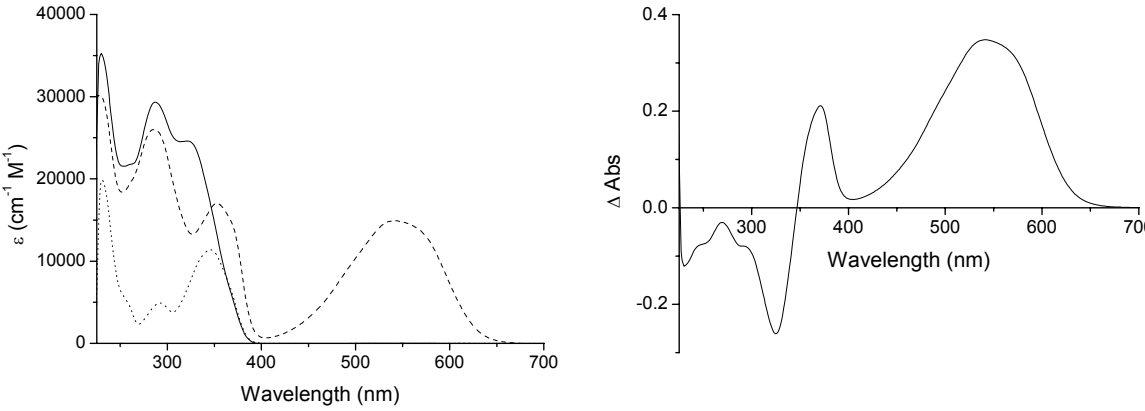

Figure 4.10 Left: UV/Vis absorption spectra of DMCS **8** in the open state (−),DMCS **8** $PSS_{365\ nm}$ (− − −) and DMCpipboc **6** (····), spectra recorded in CH_2Cl_2 at RT. Right: The UV/Vis difference spectrum for DMCS at the open and closed $PSS_{365\ nm}$ state. The spectra were recorded in CH_2Cl_2 at RT.

The difference spectra (between the open and $PSS_{365\ nm}$ states) of DMCS **8**, of PrPhSPh **10** and of MMCS **3** are similar, (Figure 4.8) confirming that the change seen in the absorption spectrum is due to the switching of the dithienylcyclopentene unit (Figure 4.10, *Right*) and, importantly, that the photochromic properties of the dithienylcyclopentene unit are unaffected by the coumarin unit in this dyad also.

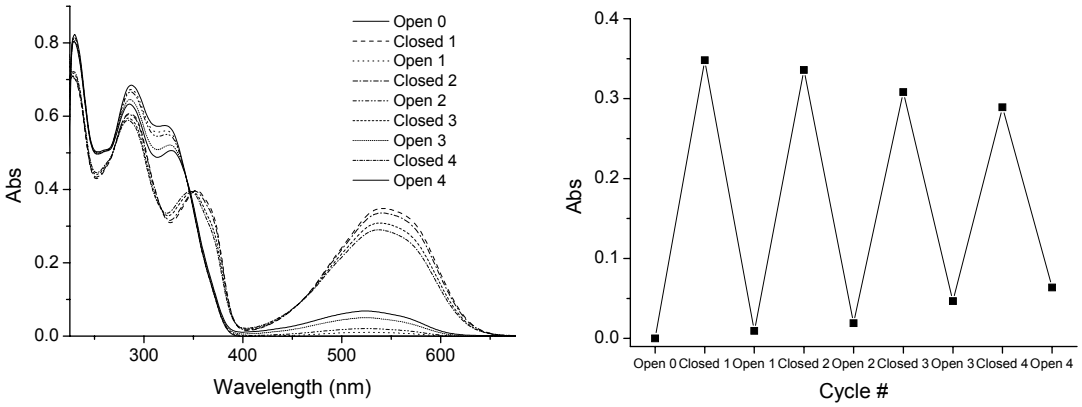

Figure 4.11 Left: UV/Vis absorption spectra of DMCS **8** recorded over several switching cycles. DMCS **8** in the open state is converted to the DMCS closed state ($PSS_{365\ nm}$) by irradiation at λ = 365 nm, the closed isomer is returned to the open state by irradiation with λ > 400 nm light. The spectra were recorded in CH_2Cl_2 at RT. Right: Absorbance at λ = 541 nm for the DMCS **8** open and $PSS_{365\ nm}$ state during four switching cycles. The spectra were recorded in CH_2Cl_2 at RT.

The photochemical switching can be performed with DMSC **8** over several open/closing cycles (Figure 4.11) and shows very efficient switching at RT with a high PSS of up to 95%, which is comparable to the switching efficiency of MMCS **3** and PrPhSPh **10**.

The emission spectra of the open form of DMCS **8** match closely that of a 1:1 mixture of the individual components **6** and **10**, showing, in contrast to MMCS **3**, that the fluorescence of the coumarin component is not quenched by the open switch. At the $PSS_{365\ nm}$ of DMCS **8**, *i.e.* in the ring closed form, a large decrease in coumarin fluorescence intensity is observed, due to quenching by the closed switch (Figure 4.12, left). This decrease in fluorescence is > 98%, *i.e.* when closed to the photostationary state using λ = 365 nm light, indicating that energy transfer to the switch is very efficient. The energy transfer quenching observed is typical for Förster resonance energy transfer,[26] which is probable considering the considerable spectral overlap of the emission spectrum of the coumarin and the absorption spectrum of the closed switch unit.

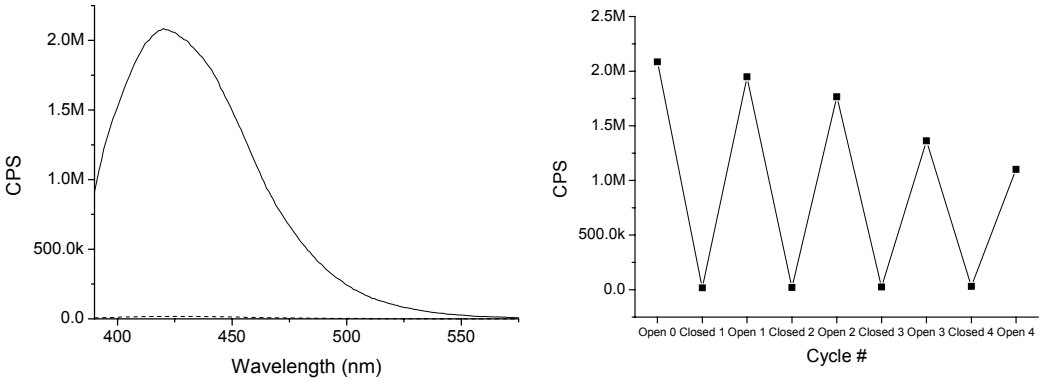

Figure 4.12 Left: fluorescence spectra (λ_{exc} = 380 nm) of DMCS **8** in the open state (−) and $PSS_{365\ nm}$ state (− − −). The spectra were compensated for absorption and recorded in CH_2Cl_2 at RT. Right: Fluorescence intensity (λ_{exc} = 380 nm) at λ = 420 nm over several switching cycles of DMCS **8** using λ = 365 nm for ring-closing and λ > 400 nm at RT for ring-opening. The spectra were recorded in CH_2Cl_2 at RT.

The switching of fluorescence was followed over four switching cycles and is found to be reversible, with high efficiency (Figure 4.12, right). However, some decrease in the maximum fluorescence for the open form is observed, probably due to an irreversible rearrangement of the closed switch, which generates a species with absorption at slightly higher energy (λ_{max} ~ 525 nm, Figure 4.12, right). The remaining absorption at shorter wavelength (*i.e.* after opening the switch with λ > 400 nm) supports the latter conclusion (see Figure 4.11). A type of rearrangement which results in this type of absorption shift was observed before by the groups of Branda and Irie.[27]

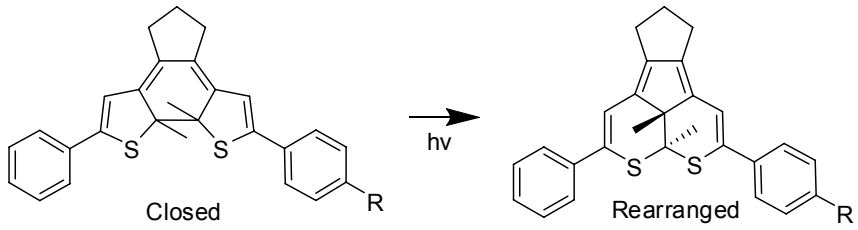

Figure 4.13 Probable side-product obtained when irradiating **8**.[27]

4.4 Redox Properties

4.4.1 MMCS 3

The redox chemistry of the open form of MMCS **3** is characterized by an irreversible oxidation at $E_{p,a}$ = 1.22 V [vs SCE], as obtained in related dithienylcyclopentene switches,[21] and an irreversible oxidation at 1.78 V [vs SCE] (not shown), the edge of the solvent window, as for MMCpipboc **9**. In the return cycle two new reduction processes are observed at potentials coincident with those of the closed form. This indicates that oxidative ring closure to MMCS(closed)$^{2+}$ is occurring. MMCS(closed)$^{2+}$ can then be reduced, first to MMCS(closed)$^{+}$ at 0.73 V and finally to MMCS(closed) at 0.40 V (Figure 4.14). Repetitive cycling results in a significant build-up of the closed form (MMCS open $\rightarrow$ closed) within the diffusion layer of the electrode, as seen in the second cycle where two new redox processes (0.48 V and 0.81 V), originating from the closed form of MMCS **3**, are observed. The electrochemical characteristics together with the absence of redox process between -2.0 V and 1.4 V for the coumarin model MMCpipboc **9**, provide compelling evidence that the oxidative processes observed are centred on the dithienylcyclopentene unit.

Table 4.2 Redox properties of the open and closed form of MMCS **3** and DMCS **8**.

	$E_{1/2}$, V vs SCE ($E_{p,a}$ where irr or qr)[a,b]	
MMCpipboc **9**	1.78 (irr)[c]	
DMCpipboc **6**	1.48 (qr)	
MMCS **3**	**Open** 1.78 (irr)[c], 1.22(irr)	**Closed** 1.78(irr)[c], 0.77, 0.43, -1.74(irr)
DMCS **8**	**Open** 1.50(qr), 1.18(irr)	**Closed** 1.50(qr), 0.78, 0.43, -1.72(irr)

[a] in CH_2Cl_2 / 0.1 M $TBAPF_6$ vs SCE [b] irr=irreversible qr = quasi reversible[28] [c]edge of solvent window.

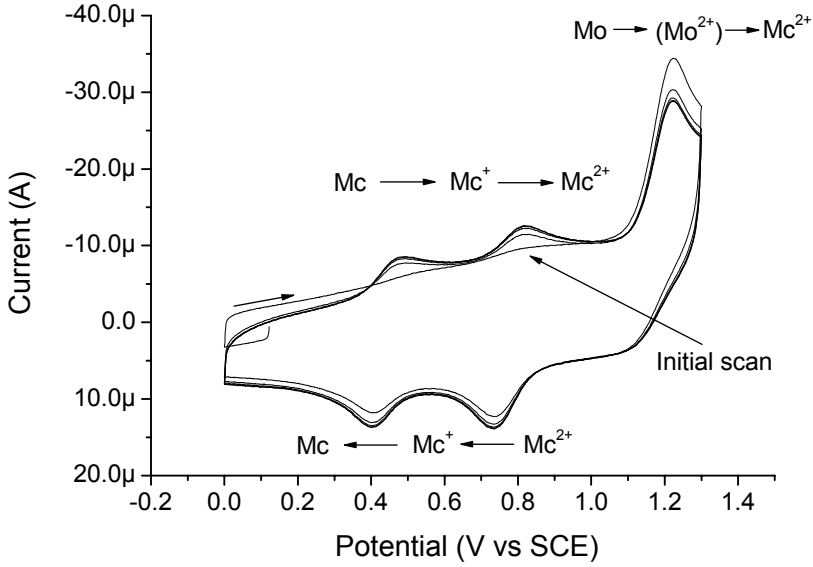

Figure 4.14 Cyclic voltammetry of the open form of MMCS **3** (Mo = MMCS open, Mc = MMCS closed) in CH_2Cl_2 / 0.1 M $TBAPF_6$ vs SCE at 1 V s^{-1}.

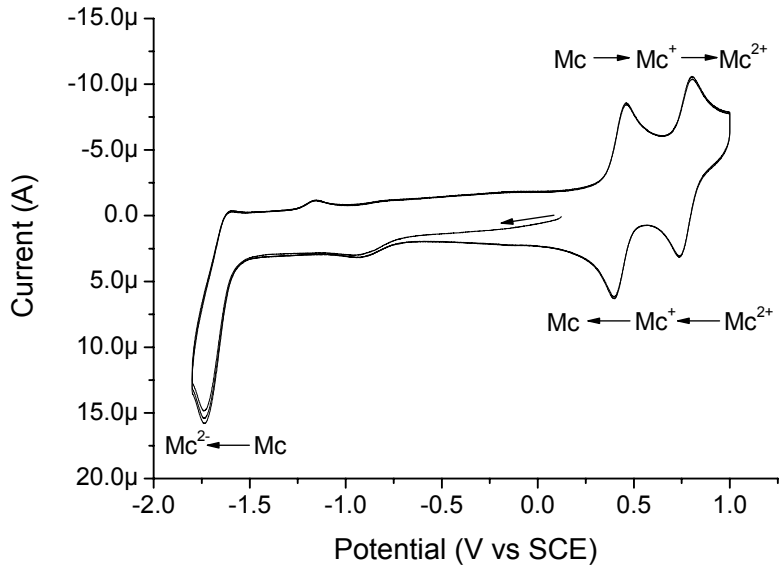

Figure 4.15 Cyclic voltammetry of the closed form of MMCS **3** (Mc) in CH_2Cl_2 / 0.1 M $TBAPF_6$ vs SCE at 0.2 V s^{-1}.

In the closed state, MMCS **3** shows less anodic redox potentials than in the open state, which indicates destabilisation of the HOMO in the closed state. For the closed form of MMCS two fully reversible oxidation processes are observed between 0.25 and 1.0 V [vs SCE], assigned to two one-electron oxidation steps (Figure 4.15). These two oxidation processes are in good agreement with the two oxidation processes that appear when oxidizing the open form and were assigned to the closed form. Similarly, two irreversible reduction steps are observed between -1.5 and -2.2 V [vs SCE] (the second reduction is not shown).

4.4.2 DMCS 8

The redox chemistry of DMCS **8** is similar to that of MMCS **3** and is characterized by an irreversible oxidation at $E_{p,a}$ = 1.18 V [vs SCE] leading to oxidative ring closure to DMCS(closed)$^{2+}$. This component can then be reduced, first to DMCS(closed)$^{+}$ at 0.74 V and finally to DMCS(closed) at 0.41 V (Figure 4.16). Also a quasi-reversible oxidation at 1.50 V [vs SCE] is observed (Figure 4.18), at the same potential as for DMCpipboc **6**. Repetitive cycling results in a significant build-up of the closed form (DMCS open → closed) in the diffusion layer of the electrode, shown in the second cycle by two new redox processes (0.46 V and 0.79 V), originating from oxidation of the closed form of DMCS **8**.

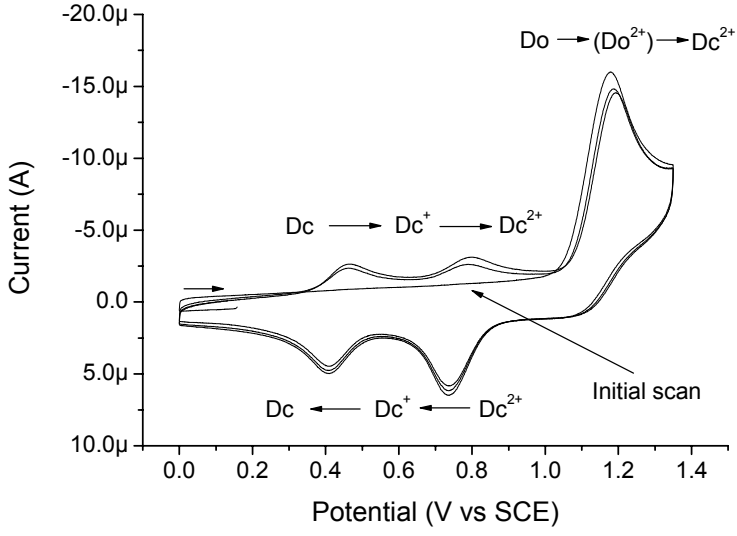

Figure 4.16 Cyclic voltammetry of the open form of DMCS **8** (DMCS open (Do), DMCS closed (Dc)) in CH_2Cl_2 / 0.1 M $TBAPF_6$ vs SCE at 0.2 V s^{-1}.

In the closed state, DMCS **8** shows less anodic redox potentials than in the open state and hence destabilisation of the HOMO. For the closed form of DMCS two fully reversible

oxidation processes are observed between 0.25 and 1.0 V (vs SCE), assigned to two one-electron oxidation steps (Figure 4.17). These two oxidation processes are in good agreement with the two oxidation processes that appear when oxidizing the open form and were assigned to the closed form, identical as observed for MMCS **3**. Similarly, two irreversible reduction steps are observed between -1.5 and -2.2 V [vs SCE] (not shown).

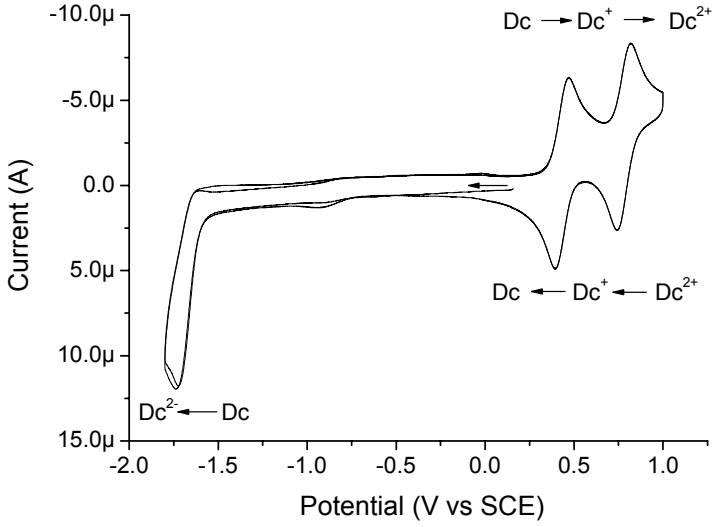

Figure 4.17 Cyclic voltammetry of the closed form of DMCS **8** (Dc) in CH_2Cl_2 / 0.1 M $TBAPF_6$ vs SCE at 0.1 V s^{-1}.

When the potential window is extended to 1.5V [vs SCE] another quasireversible redox wave is observed for DMCS(closed)$^{2+}$ → DMCS(closed)$^{3+}$, due to oxidation of the coumarin moiety (also observed for the coumarin model DMCpipboc **6**, not shown). This third oxidation makes the cation insoluble in CH_2Cl_2 and results in its precipitation on the electrode surface. As a result on the subsequent cathodic sweep a surface confined (non-diffusion dependent) process takes place, observed as a desorption spike at 0.68 V, where the precipitated polycationic molecules are reduced to the better soluble DMCS(closed)$^{1+}$ state, allowing it to desorb from the surface of the electrode and return to solution (Figure 4.18). This shows that it is important to stay away from the coumarin oxidation when closing the switch by cyclic voltammetry, since adsorption on the surface of the electrode might hinder the closing process for the diarylcyclopentene switches which are still in solution.

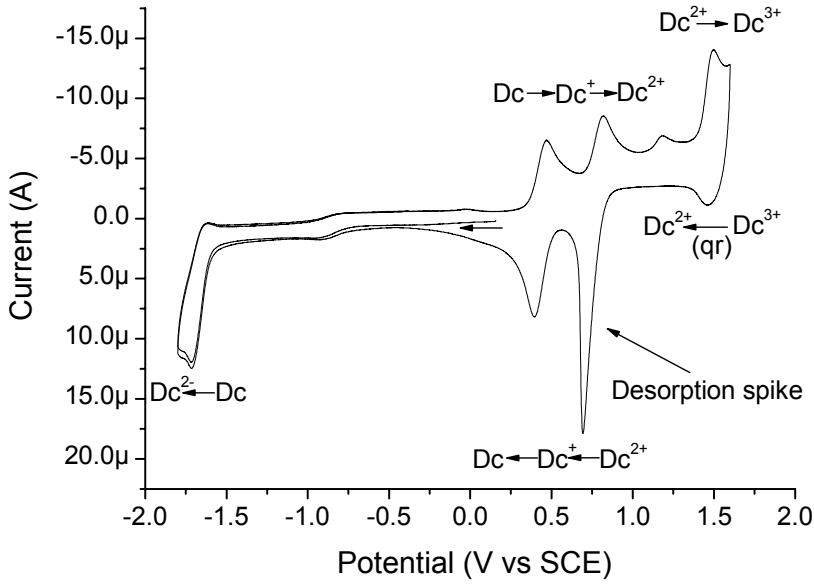

Figure 4.18 Cyclic voltammetry of the closed form of DMCS **8** (Dc) in CH_2Cl_2 / 0.1 M $TBAPF_6$ vs SCE at 0.1 V s^{-1}.

4.5 Spectroelectrochemistry

In order to further investigate the possibility of opening and closing the switch by cyclic voltammetry and thereby to be able to use is as an "electrochemical" fluorescence switch, the system was investigated using spectroelectrochemistry. The investigation showed similar behaviour as for phenyl and *p*-methoxyphenyl substituted dithienylcyclopentene, which were investigated previously within our group.[21] When a solution of DMCS **3** in CH_2Cl_2 is subjected to a constant potential of 1.2 V [vs Ag/Ag^+] the absorption spectrum shows similar changes as observed for the phenyl substituted dithienylcyclopentene (Figure 4.19). During the first phase (1) the formation of $DMCS^{2+}$ closed (Dc^{2+}) from DMCS open (λ_{max} at 432 and 566 nm) is accompanied by some formation of the monocation (Dc^+, λ_{max} at 758 nm). After oxidation the slow formation of an unidentified species Dx is observed (peak at 646 nm). Once all DMCS open has been transformed into Dc^{2+} and the electrolysis is stopped, the amount of Dc^{2+} starts to decrease while the amount of Dc^+ remains constant. During this period the amount of Dx steadily increases. After 20 min a steady state is reached were the amount of Dc^{2+} and Dc^+ reaches a minimum and for Dx a maximum amount is observed (Figure 4.19, state 3). The formation of Dx, which occurs when electrochemically closing the switch in solution, is problematic since it is, therefore, not

possible to reach a fully closed state (i.e. only Dc^{2+}) and thereby electrochemically switch from the open to the closed form. However, this behaviour is fully consistent with a previous study in solution of the switching unit.[21] It was already shown by Areephong *et al.* that it is possible to electrochemically switch these dithienylcyclopentenes when they are connected to a surface.[19] This results show that if we want an electrochemically controllable fluorescence switch (i.e. that can be reversibly opened and closed) the next step would need to be towards a functionalised surface.

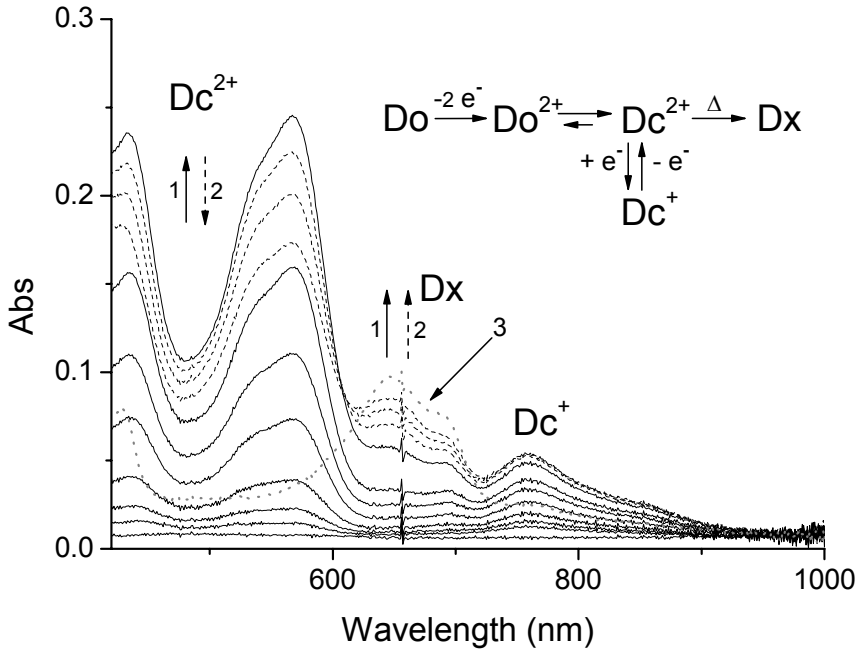

Figure 4.19 Spectroelectrochemistry of DMCS **3** in the open state during phase (1) (−), phase (2), no electrolysis (- - -) and the final state (3) (····). During 20 min at 1.2 V vs Ag/Ag^+ in CH_2Cl_2 / 0.1 M $TBAPF_6$ at RT.

4.6 Excited state dynamics

4.6.1 MMCS 3

Time-correlated single photon counting (TCSPC) measurements were performed on the open form and closed form ($PSS_{365\ nm}$) of MMCS **3**. In the open state, the emission decay of the MMCS **3** (λ_{exc} = 337 nm, λ_{em} = 420 nm) is cross-correlated with the excitation pulse and the process has a fluorescence lifetime of lower than ~ 200 ps (Figure 4.20, left). This decay lifetime is due to the quenching of the coumarin excited state by energy transfer, most likely by a Dexter type mechanism (*vide infra*). At the $PSS_{365\ nm}$ state in which a mixture of the open and closed form of the switch is present, even though the PSS equilibrium of MMCS **3** is largely towards the closed form (>95%), the emission decay shows a long 2.0 ns and a short < 200 ps contribution to the decay (Figure 4.20, right).

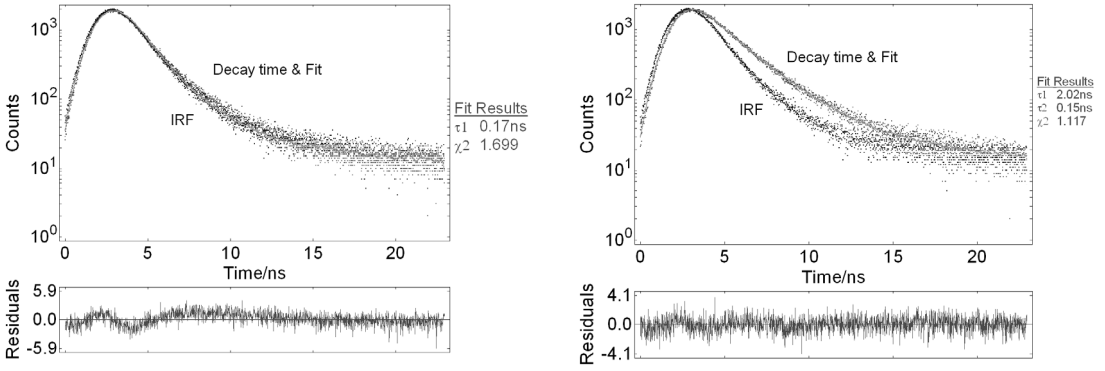

Figure 4.20 Left: TCSPC spectrum of MMCS **3** (open state) with: the decay trace of MMCS open, the fit to the fluorescence decay and IRF: the instrument response function. Right: TCSPC spectrum of MMCS ($PSS_{365\ nm}$) with: the decay trace of MMCS $PSS_{365\ nm}$, the fit to the fluorescence decay and IRF: the instrument response function.

The short contribution can be attributed to the residual coumarin emission during the lifetime of energy transfer from the coumarin to the closed dithienylcyclopentene unit. The long lifetime, which only has a small overall contribution to the trace, is most likely due to "free" coumarin, which is formed upon irradiation by degradation of the dithienylcyclopentene unit itself, thereby eliminating the quenching effect and allowing emission from a small amount of the coumarin. This conclusion is supported by a similar fluorescence decay lifetime for MMCpipboc **9** (1.4 ns). Overall the bulk of the energy

absorbed by the coumarin is quenched by another component, most likely by the dithienylcyclopentene, in both the open *and* the closed state of MMCS **3**.

4.6.2 DMCS 8

Time correlated single photon counting (TCSPC) measurements were performed on the open form and closed form ($PSS_{365\ nm}$) state of DMCS. In the open state, the time profile of the emission of the DMCS (λ_{exc} = 337 nm, λ_{em} = 420 nm) shows a long decay component of 2.3 ns, which is in good agreement with the fluorescence lifetime of DMCpipboc **6** (2.7 ns). Therefore, this long decay component is assigned to the dimethoxy coumarin connected to the open form of the dithienylcyclopentene switch (Figure 4.21, left). A short decay component, which is cross-correlated with the excitation pulse, can be observed and this process has a fluorescence lifetime of lower than ~ 200 ps. This fast decay, which is a minor component, is assigned to energy transfer of the coumarin to the small amount of closed form of the dithienylcyclopentene present in solution.[29]

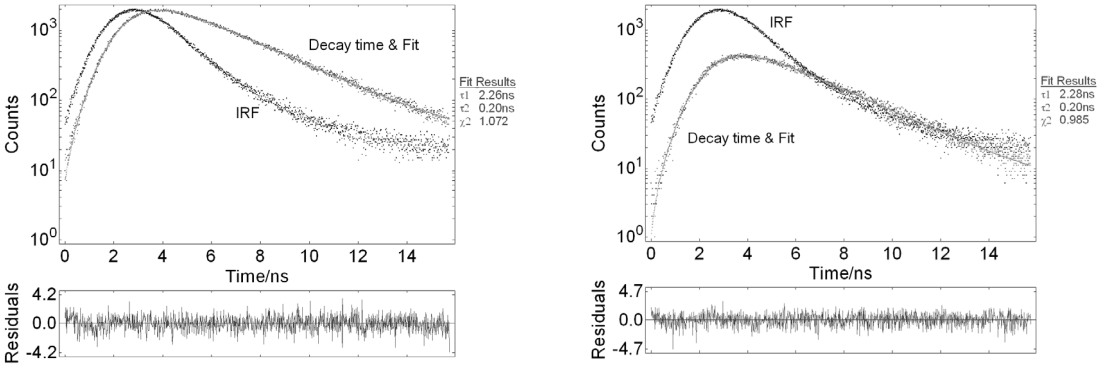

Figure 4.21 Left: TCSPC spectrum of DMCS **8** open with: the decay trace of DMCS open, the fit to the fluorescence decay recorded at λ_{em} = 420 nm for 10 min and IRF: the instrument response function green. Right: TCSPC spectrum of DMCS closed ($PSS_{365\ nm}$) with: the decay trace of DMCS $PSS_{365\ nm}$, green the fit to the fluorescence decay recorded at λ_{em} = 420 nm for 10 min blue, and the instrument response function.

At the $PSS_{365\ nm}$ state, in which a mixture of the open and closed form (>95% of closed form) of the switch **8** is present, the emission decay lifetimes were assigned as in the open form, however, the overall intensity has decreased (both spectra were obtained over 10 min accumulation time) (Figure 4.21, right). This indicates that the fluorescence lifetime of the dimethoxy coumarin remains the same (i.e. in the remaining open form) and the rate of energy transfer has not changed (i.e. the short component still has the same lifetime, ~ 200 ps), but also that part of the energy is being transferred elsewhere (since there are less

counts coming from the coumarin than in the open form), in this case being quenched by the closed form of the switch (short component).

The reversibility of the switching process fluorescence quenching can be followed using TCSPC by recording the decay traces over a set period of time, in this case 10 min. The low intensity irradiation used during the TCSPC assures that the state of the DMCS **8** solution (i.e. open or PSS_{365nm}) is not changed during data acquisition (Figure 4.22). The open form of DMCS **8** can be irradiated to the closed form ($PSS_{365\ nm}$), then reopened using $\lambda > 400$ nm and finally irradiated again to the closed form of **8** ($PSS_{365\ nm}$). During this process the observed fluorescence output (*e.g.* counts per 10 min) is modulating, indicating that in the $PSS_{365\ nm}$ state of **8** the energy of the dimethoxy coumarin is being quenched by the closed form of the dithienylcyclopentene. The change in the extent of fluorescence quenching is reversible,[30] confirming that it is not due to photodegradation but due to the appearance and disappearance of the low energy absorption band of the closed dithienylcyclopentene.

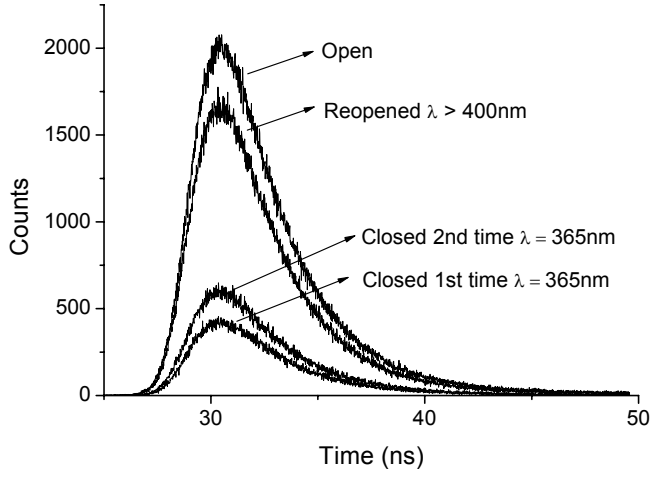

Figure 4.22 TCSPC spectra of DMCS **8**, open and closed forms ($PSS_{365\ nm}$). PSS obtained by irradiating with $\lambda = 365$ nm light and the open form of DMCS obtained after irradiating the closed form ($PSS_{365\ nm}$) form with $\lambda > 400$ nm light for 20 min. Fluorescence decay counts measured at $\lambda_{em} = 420$ nm for 10 min; all traces recorded in CH_2Cl_2 at RT.

4.7 Discussion

Two structurally similar coumarin donor – dithienylcyclopentene acceptor diads have been prepared and characterized by NMR and mass spectroscopy, i.e. MMCS **3** and DMCS **8**, which differ only in the substitution pattern of the coumarin unit. This change in structure causes a bathochromic shift in the λ_{max} of absorption from the monomethoxy coumarin to dimethoxy coumarin. A corresponding shift is observed in the emission properties of both coumarins and as a consequence the photophysical behaviour of both dyads (i.e. MMCS **3** and DMCS **8**) is remarkably different.

The absorption spectrum of the monomethoxy switch shows the spectral features of both MMCpipboc **9** and dithienylcyclopentene (Figure 4.9, right). When irradiated at λ = 365 nm the dithienylcyclopentene unit of MMCS **3** undergoes photochemical ring closure, which results in the appearance of a lower energy absorption at λ_{max} = 540 nm. This photochemical ring closure reaches a very high PSS comprising > 95% of the closed form of **3** and also shows good stability at RT over several switching cycles. The initial concept was to use the appearance of this lower energy absorption band to quench the coumarin excited state. However, when considering the emission spectra of the open state and PSS of the MMCS **3** the fluorescence spectrum observed is of very low intensity compared with an equimolar coumarin model MMCpipboc **9** solution (Figure 4.9, Right). Surprisingly, in both the open state and the PSS, the excited state energy of the coumarin is quenched. This is indicated also by the large contribution of the short lifetime component (< 200 ps) observed with TCSPC for both the open and the closed state of **3** ($PSS_{365\ nm}$).

In order to understand why this coumarin was not energetically compatible with the diphenyl dithienylcyclopentene, the absorption spectrum of the coumarin was compared with that of the model switch, PrPhSPh **10** (Figure 4.23). The absorption spectrum of PrPhSPh **10** overlaps fully with that of MMCpipboc and the lowest energy absorption is attributable to the dithienylcyclopentene unit and not to the coumarin. This situation makes it likely that the energy levels of the coumarin and switch unit are in a range compatible with Dexter type energy transfer, which requires overlap in wavefunction for the energy donor (i.e. the monomethoxy coumarin) and the energy acceptor (i.e. the dithienyl cylopentene). When an alternative coumarin is employed (i.e. DMCpipboc **6**) the absorption of the open form of the dithienylcyclopentene is no longer the lowest energy absorption. Instead the dimethoxy coumarin is lowest in energy, thereby allowing the observation of coumarin emission in the open form.

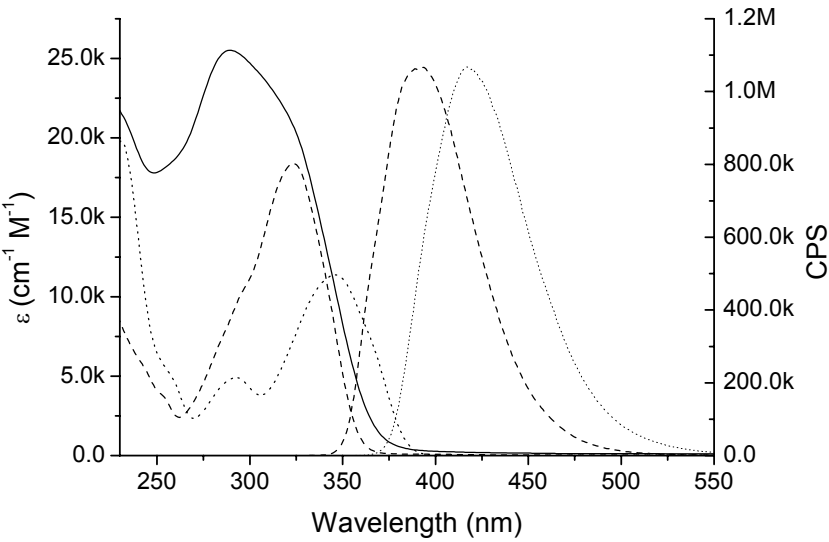

Figure 4.23 Absorption spectra of PrPhSPh **10** (−), MMCpipboc **9** (−−−) and DMCpipboc **6** (····). On the right side the normalized fluorescence spectra for MMCpipboc **9** (−−−) and DMCpipboc **6** (····) are also shown. The spectra were recorded in CH_2Cl_2 at RT.

The diphenyl dithienylcyclopentene substituted with the dimethoxy coumarin (DMCS **8**) shows identical switching properties compared to the MMCS **3**, with good stability and high switching efficiency (i.e. high PSS). In this compound, however, the open form of the DMCS **8** shows a strong emission at the same wavelength as the coumarin (i.e. DMCpipboc **6**) emission (Figure 4.12) and the fluorescence decay lifetime observed for this emission is in good agreement to that of the free coumarin (2.7 ns). Irradiation of DMCS **8** to the closed form using λ = 365 nm light, results in the emission at λ = 420 nm decreasing in intensity by more then 98%. Due to the overlap of the emission band of the coumarin with the low energy absorption band ($\lambda \sim 540$ nm) of the closed form of the dithienylcyclopentene unit, the quenching is assigned to a Förster type mechanism. Fluorescence decay lifetime measurements at the PSS state still show a minor contribution of the longer lifetime (i.e. DMCpipboc **6**) component, but the largest contribution is due to a < 200 ps component, which can be attributed to the quenched emission of the coumarin by the closed dithienylcyclopentene, as was observed for the MMCS also. Opening the closed dithienylcyclopentene using λ > 400 nm light results in almost full recovery of the fluorescence output and this can be repeated over several switching cycles (Figure 4.12, right). This shows that the electronic properties of the coumarin donor have been

sufficiently altered to inhibit quenching by the dithienylcyclopentene open form and to allow for quenching only in the closed state by Förster resonance energy transfer.

The redox properties of the individual units of MMCS **3** and DMCS **8**, determined by cyclic voltammetry, give a good indication of the differences in HOMO and LUMO levels in the two compounds. For the diphenyl dithienylcyclopentene unit the properties are the same for the three compounds (i.e. PrPhSPh **10**, MMCS **3** and DMCS **8**), as both first oxidation and first reduction take place at identical potentials (vs SCE). For the mono and dimethoxy coumarin (quasi)irreversible oxidations are observed at 1.6 V and 1.8 V (vs SCE) respectively. This shows that the different substitution pattern (i.e. the extra methoxy group) destabilises the HOMO level of the coumarin and brings it closer to the LUMO, thereby decreasing the bandgap and causing a bathochromic shift in the absorption spectrum for the DMCpipboc **6**.

4.8 Conclusions

Investigation of MMCS **3** and DMCS **8** shows that by small changes to the relative energy levels of two components it is possible to change from a Dexter energy transfer mechanism to a Förster mechanism. In the present case, the introduction of an additional methoxy substituent, transforms a barely fluorescent photochromic switch (MMCS **3**) into a molecule with up to 98% switchable fluorescence (DMCS **8**). Using cyclic voltammetry it is also possible to close the dithienylcyclopentene switch in solution showing that the electrochemical properties of the switching unit are unaffected by the attachment of the fluorophore. On a surface it is has been shown earlier that it is possible to both open *and* close the dithienylcyclopentene unit electrochemically.[19] Combining the fluorescence switching properties of DMCS **8** in solution with the reversible switching of dithienylcyclopentenes on an ITO surface, opens the possibility of electro- and photo-chemical control of fluorescence output.

4.9 Experimental section

For all spectroscopic measurements Uvasol-grade solvents (Merck) were employed. All reagents employed in synthetic procedures were of reagent grade or better, and used as received unless stated otherwise. Jetsuda Areephong is acknowledged for providing compounds **1** and **10**.[19] Compounds **2**[20], **4**[23] and **5**[31] were prepared according to literature. ^{1}H NMR spectra were recorded at 200, 300, or 400 MHz; ^{13}C NMR spectra at 50.3, 75.4 or 125.7 MHz. All spectra were recorded at ambient temperature, with the residual proton signals of the solvent as an internal reference. Chemical shifts are reported in ppm relative to TMS. CI and EI mass spectra were recorded on a Jeol JMS-600 mass spectrometer in the scan range of m/z 50–1000 with an acquisition time between 300 and 900 ms and a

potential between 30 and 70 V. MALDI-TOF spectra were recorded on an Applied Biosystems Voyager-DE Pro. UV/Vis absorption spectra (accuracy ±2 nm) were recorded on a Hewlett-Packard UV/Vis 8453 spectrometer. The fluorescence measurements were performed on a SPF-500C spectrofluorometer manufactured by SLM Aminco, and a Jobin-Yvon Fluorolog 3-22, the sharp features between λ = 450 and 500 nm in the excitation spectra are instrumental artefacts, the excitation and emission spectra are uncorrected for variations in lamp intensity and detector response. Sample concentration typically 10^{-5} M, spectra were recorded in 10 mm pathlength quartz fluorescence cuvettes.

Electrochemical measurements were carried out on a Model 630B Electrochemical Workstation (CHInstruments). Analyte concentrations were typically 0.5–1 mM in anhydrous dichloromethane containing 0.1 M TBAP. Unless otherwise stated, a Teflon-shrouded glassy carbon working electrode (CHInstruments), a Pt wire auxiliary electrode and SCE or nonaqueous Ag/Ag^+ ion reference electrode were employed. Reference electrodes were calibrated with 0.1 mM solutions of ferrocene (0.38 V versus SCE in 0.1 M TBAP/ CH_3CN). Solutions for reduction measurements were deoxygenated by purging with dry N_2 gas (presaturated with solvent) prior to the measurement. Cyclic voltammograms were obtained at sweep rates of between 10 mVs^{-1} and 50 Vs^{-1}; differential pulse voltammetry (DPV) experiments were performed with a scan rate of 20 mVs^{-1}, a pulse height of 75 mV and a duration of 40 ms. For reversible processes the half-wave potential values are reported; identical values were obtained from DPV and CV measurements. Redox potentials are given with an accuracy of ±10 mV.

Luminescence lifetime measurements were obtained using an Edinburgh Analytical Instruments (EAI) time-correlated single-photon counting apparatus (TCSPC) comprised of two model J-yA monochromators (emission and excitation), a single photon photomultiplier detection system model 5300, and a F900 nanosecond flashlamp (N_2 filled at 1.1 atm pressure, 40 kHz) interfaced with a personal computer via a Norland MCA card. A 400 nm cut off filter was used in emission to attenuate scatter of the excitation light (337 nm). Data correlation and manipulation was carried out using EAI F900 software version 5.1.3. Emission lifetimes were calculated using a single-exponential fitting function, Levenberg-Marquardt algorithm with iterative deconvolution (Edinburgh instruments F900 software). The reduced χ^2 and residual plots were used to judge the quality of the fits. Lifetimes are given with an accuracy of ± 5%.

(3) 7-Methoxy-3-{2-[4-(4-{5-methyl-4-[2-(2-methyl-5-phenyl-thiophen-3-yl)-cyclopent-1-enyl]-thiophen-2-yl}-benzoyl)-piperazin-1-yl]-2-oxo-ethyl}-chromen-2-one (MMCS)

Mono carboxylic acid **1** (100 mg, 0.22 mmol) was suspended in CH_2Cl_2 (20 ml) and placed in an ice bath. Subsequently N-methylmorpholine (25 mg, 0.24 mmol) was added. After the compounds dissolved 2-chloro-4,6-dimethoxytriazine (42 mg, 0.24 mmol) was added. The reaction mixture was stirred for 4h at 0 °C, after which one equivalent of N-methylmorpholine (25 ml, 0.24 mmol) was added followed by **2** (73 mg, 0.24 mmol). Stirring was continued for 1h at 0 °C, followed by stirring overnight at room temperature. CH_2Cl_2 (50 ml) was added and the solution was washed with, respectively, 1 M aq. HCl (2 x 20 ml), brine (1x 20 ml), saturated aqueous bicarbonate solution (1 x 20 ml) and H_2O (1 x 20 ml). The organic phase was dried on Na_2SO_4, filtered and the solvent evaporated. The resulting solid was purified using column chromatography (2% MeOH in CH_2Cl_2, SiO_2), yielding **3** as a white solid (44 mg, 0.059 mmol, 26.8 %). m.p. 106.9 – 107.4 ^oC. ^1H NMR (400 MHz, $CDCl_3$) δ = 7.69 (s, 1H), 7.56-7.46 (m, 4H), 7.42-7.29 (m, 5H), 7.25-7.19 (m, 1H), 7.08 (s, 1H), 7.04 (s, 1H), 6.88-6.79 (m, 2H), 3.87 (s, 3H), 3.69 (bs, 8H), 3.60 (bs, 2H), 2.85 (t, J = 7.4 Hz, 4H), 2.14-2.04 (m, 2H), 2.02 (s, 3H), 1.99 (s, 3H) ppm. ^{13}C NMR (101 MHz, $CDCl_3$) δ = 170.54 (s), 168.78 (s), 162.75 (s), 162.18 (s), 155.44 (s), 142.27 (d), 139.97 (s), 138.54 (s), 137.22 (s), 136.78 (s), 136.57 (s), 135.90 (s), 135.26 (s), 134.71 (s), 134.67 (s), 134.60 (s), 133.35 (s), 129.02 (d), 128.84 (d), 128.15 (d), 127.22 (d), 125.52 (d), 125.43 (d), 125.26 (d), 124.15 (d), 119.52 (s), 113.13 (s), 112.98 (d), 100.80 (d), 56.00 (q), 46.45 (t), 42.34 (t), 38.69 (t), 38.64 (t), 34.31 (t), 23.25 (t), 14.76 (q), 14.65 (q) ppm. MALDI-TOF MS (MW = 740.24) m/z = 740.47 [M^+].

(6) 4-[2-(6,7-Dimethoxy-2-oxo-2*H*-chromen-4-yl)-acetyl]-piperazine-1-carboxylic acid *tert*-butyl ester (DMCpipBoc)

6,7-Dimethoxycoumarin-4-acetic acid **4** (1.0 g, 3.8 mmol) was suspended in 50 ml of CH_2Cl_2 and stirred under nitrogen atmosphere. N,N'-Carbonyldiimidazole (CDI) (665 mg, 4.1 mmol) was added and the reaction mixture was stirred under N_2 till all CO_2 had evolved and stirring continued for another 30 min. *N*-Boc-piperazine **5** (775 mg, 4.1 mmol) was added and the reaction mixture was stirred under N_2 at RT overnight. The reaction mixture was then extracted twice with 1M HCl (aq), once with water and twice with 5% $NaHCO_3$ (aq). The organic phase was then dried over Na_2SO_4, filtered and the solvent evaporated. The crude mixture was purified using column chromatography (2% MeOH in CH_2Cl_2) giving **6** as a yellow solid (1.1 g, 2.4 mmol, 63.2%). m.p. 197.1 – 197.8 ^oC. ^1H NMR (400 MHz, $CDCl_3$) δ = 7.01 (s, 1H), 6.76 (s, 1H), 6.10 (s, 1H), 3.87 (s, 3H), 3.85 (s, 3H), 3.79 (s, 2H), 3.60-3.54 (m, 2H), 3.48-3.41 (m, 2H), 3.41-3.33 (m, 4H), 1.40 (s, 9H) ppm. ^{13}C NMR (101 MHz, $CDCl_3$) δ = 166.5 (s), 160.8 (s), 154.2 (s), 152.9 (s), 149.5 (s), 149.3 (s), 146.1

(s), 112.8 (d), 111.3 (s), 105.3 (d), 99.9 (d), 80.3 (s), 56.3 (q), 56.2 (q), 45.9 (t), 43.4 (t), 41.7 (t), 37.9 (t), 28.2 (q) ppm. MS(EI) for $C_{22}H_{28}N_2O_7$ m/z 432 [M^+], HRMS calcd for $C_{22}H_{28}N_2O_7$: 432.190, found: 432.188.

General deprotection method for *N*-BOC protected amines:

The Boc protected amine was stirred in a mixture of 1:1 CH_2Cl_2 : CF_3COOH for 4h. An equal amount of water was added and the mixture was neutralized by adding solid $NaHCO_3$, after which the aqueous layer was separated and the organic layer was washed with saturated $NaHCO_3$ solution. Subsequently, the organic layer was dried over Na_2SO_4 and the solvent evaporated. The resulting product was used in subsequent steps without further purification.

(8) 6,7-Dimethoxy-4-{2-[4-(4-{5-methyl-4-[2-(2-methyl-5-phenyl-thiophen-3-yl)-cyclopent-1-enyl]-thiophen-2-yl}-benzoyl)-piperazin-1-yl]-2-oxo-ethyl}-chromen-2-one (DMCS)

This compound was synthesized using a procedure similar to the one used for MMCS **3** using **1** (200 mg 0.44 mmol) and **7** (from **6** deprotected using the general method) (162 mg, 0.48 mmol). Purification gave **8** (158 mg, 0.20 mmol, 45.5%). m.p. 201.6 – 202.0 ^oC. ^1H NMR (400 MHz, $CDCl_3$) δ = 7.54-7.45 (m, 4H), 7.39-7.29 (m, 4H), 7.25-7.19 (m, 1H), 7.07 (s, 2H), 7.03 (s, 1H), 6.84 (s, 1H), 6.16 (s, 1H), 3.94 (s, 3H), 3.91 (s, 3H), 3.84 (s, 2H), 3.68 (s, 4H), 3.55 (s, 4H), 2.84 (t, J = 7.43 Hz, 4H), 2.13-2.04 (m, 2H), 2.02 (s, 3H), 1.98 (s, 3H) ppm. ^{13}C NMR (101 MHz, $CDCl_3$) δ = 170.59 (s), 166.97 (s), 161.10 (s), 153.41 (s), 149.98 (s), 149.39 (s), 146.57 (s), 139.96 (s), 138.41 (s), 137.26 (s), 136.78 (s), 136.74 (s), 136.01 (s), 135.30 (s), 134.70 (s), 134.65 (s), 134.56 (s), 133.00 (s), 129.03 (d), 128.17 (d), 127.24 (d), 125.50 (d), 125.46 (d), 125.35 (d), 124.14 (d), 113.20 (d), 111.58 (s), 105.67 (d), 100.46 (d), 56.76 (q), 56.64 (q), 46.49 (t), 42.40 (t), 38.69 (t), 38.63 (t), 38.36 (t), 23.25 (t), 14.77 (q), 14.65 (q). ppm. MALDI-TOF MS (MW = 770.3) m/z = 770.4 [M^+].

4.10 References

1 W. M. Moreau, *Semiconductor Lithography*, Plenum Press, New York, **1988**.

2 http://en.wikipedia.org/wiki/Magnetic_storage

3 http://en.wikipedia.org/wiki/Optical_data_storage

4 (a) J. E. Green, J. W. Choi, A. Boukai, Y. Bunimovich, E. Johnston-Halperin, E. Delonno, Y. Luo, B. A. Sheriff, K. Xu, Y. S. Shin, H. R. Tseng, J. F. Stoddart and J. R. Heath, *Nature* **2007**, *445*, 414-417. (b) A. P. de Silva, M. R. James, B. O. F. McKinney, D. A. Pears and S. M. Weir, *Nat. Mater.* **2006**, *5* , 787-790.

5 B. L. Feringa, Ed. Molecular Switches (Wiley VCH, Weinheim, **2001**).

6 Y. Yokoyama, *Chem. Rev.* **2000**, *100* (5), 1717-1739.

7 G. Berkovic, V. Krongauz and V. Weiss, *Chem. Rev.* **2000**, *100*, 1741-1753.

8 (a) H. Tian and S. J. Yang, *Chem. Soc. Rev.* **2004**, *33*, 85-97. (b) M. Irie, *Chem. Rev.* **2000**, *100*, 1685-1716.

9 (a) S. Abad, M. Kluciar, M. A. Miranda and U. Pischel, *J. Org. Chem.* **2005**, *70*, 10565-10568. (b) S.A. de Silva, K. C. Loo, B. Amorelli, S. L. Pathirana, M. Nyakirang'ani, M. Dharmasena, S. Demarais, B. Dorcley, P. Pullay and Y. A. Salih, *J. Mater. Chem.* **2005**, *15*, 2791-2795.

10 A. Peters and N. R. Branda, *Chem. Commun.*, **2003**, 954.

11 A. Momotake and T. Arai, *J. Photoch. Photobio. C* **2004**, *5*, 1-25.

12 (a) K. Matsuda and M. Irie, *J. Photoch. Photobio. C* **2004**, *5*, 169-182. (b) F. M. Raymo, and M. Tomasulo, *Chem. Soc. Rev.* **2005**, *34*, 327-336. (c) F. M. Raymo and M. Tomasulo, *J. Phys. Chem. A* **2005**, *109*, 7343-7352. (d) F. M. Raymo and M. Tomasulo, *Chem. Eur. J.* **2006**, *12*, 3186-3193.

13 A. Fernandez-Acebes and J. M. Lehn, *Chem. Eur. J.* **1999**, *5*, 3285-3292.

14 (a) M. Irie, T. Fukaminato, T. Sasaki, N. Tamai and T. Kawai, *Nature* **2002**, *420*, 759-760. (b) T. Fukaminato, T. Sasaki, T. Kawai, N. Tamai and M. Irie, *J. Am. Chem. Soc.* **2004**, *126*, 14843-14849. (c) L. Giordano, T. M. Jovin, M. Irie and E. A. Jares-Erijman, *J. Am. Chem. Soc.* **2002**, *124*, 7481-7489.

15 (a) S. Wang, W. Shen, Y. L. Feng and H. Tian, *Chem. Commun.* **2006**, 1497-1499. (b) G. Y. Jiang, S. Wang, W. F. Yuan, L. Jiang, Y. L. Song, H. Tian and D.B. Zhu, *Chem. Mater.* **2006**, *18*, 235-237.

16 T. B. Norsten and N. R. Branda, *J. Am. Chem. Soc.* **2001**, *123*, 1784-1785.

17 (a) R. T. F. Jukes, V. Adamo, F. Hartl, P. Belser, L. De Cola, *Inorg. Chem.* **2004**, *43*, 2779-2792. (b) T. A. Golovkova, D. V. Kozlov and D. C. Neckers, *J. Org. Chem.* **2005**, *70*, 5545-5549.

18 J. J. D. de Jong, L. N. Lucas, R. Hania, A. Pugzlys, R. M. Kellogg, B. L. Feringa, K. Duppen and J. H. van Esch, *Eur. J. Org. Chem.* **2003**, 1887-1893.

19 J. Areephong, W. R. Browne, N. Katsonis and B. L. Feringa, *Chem. Commun.* **2006**, 3930-3932.

20 J.H. Hurenkamp, W.R. Browne, R. Augulis, A. Pugžlys, P.H.M. van Loosdrecht, J.H. van Esch and B.L. Feringa, *Org. Biomol. Chem.* **2007**, *5*, 3354-3362.

21 (a) W. R. Browne, J. J. D. de Jong, T. Kudernac, M. Walko, L.N. Lucas, K. Uchida, J.H. van Esch and B.L. Feringa, *Chem. Eur. J.* **2005**, *11*, 6414-6429. (b) W. R. Browne, J. J. D. de Jong, T. Kudernac, M. Walko, L.N. Lucas, K. Uchida, J.H. van Esch and B.L. Feringa, *Chem. Eur. J.* **2005**, *11*, 6430-6441.

22 (a) J. J. D. de Jong, L. N. Lucas, R. M. Kellogg, J.H. van Esch and B.L. Feringa, *Science* **2004**, *304*, 278-281 (b) Ph.D. Thesis L. N. Lucas, Towards Photoresponsive Supramolecular Materials, University of Groningen, **2001**, ISBN 90-367-1528-8.

23 Y. Ma, W. Luo, P. J. Quinn, Z. Liu and R. C. Hider, *J. Med. Chem.* **2004**, *47*, 6349-6362

24 G. Anderson and R. Paul, *J. Am. Chem. Soc.*, **1958**, *80*, 4423-4423

25 λ = 365 nm was chosen as irradiation wavelength since it lies at the edge of the open switch **10** absorption and UV irradiation of that wavelength gives little degradation.

26 N. J. Turro, *Modern Molecular Photochemistry* (University Science Books, Sausalito, **1991**)

27 (a) A. Peters and N. R. Branda, *Adv. Mater. Opt. Electron.* **2000**, *10* (6), 245-249. (b) M. Irie, T. Lifka, K. Uchida, S. Kobatake and Y. Shindo, *Chem. Commun.* **1999**, (8), 747-748.

28 Here, quasireversibility and irreversibility refer to the chemical stability of the oxidised or reduced species. In all cases electrochemical reversibility ($E_{p,a}$ -$E_{p,c}$< 80 mV) is observed between 0.01 and 2.0 Vs^{-1}, where the chemical stability of the oxidised/reduced species is sufficient to observe the return wave. Where the $I_{p,a}$ peak is not significantly different to the $I_{p,c}$ peak, the term reversible is applied; similarly, quasireversiblity refers to situations in which chemical reversibility is dependent on scan rate (i.e. reversibility is observed only at higher scan rates).

29 The diphenyldithienylcyclopentene switches are very sensitive to irradiation, it is close to impossible to exclude all light while performing these experiments.

30 A UV/Vis spectrometer was not available at the time of the measurements, hence the lack of full reversibility is due to the fact that it was not possible to confirm the full re-opening/closing of the switch,

31 (a) E. A. A. Wallén, J. A. M. Christiaans, E. M. Jarho, M. M. Forsberg, J. I. Venäläinen, P. T. Mannisto and J. Gynther, *J. Med. Chem.* **2003**, *46*, 4543-4551. (b) L. A. Carpino, E. M. E. Mansour, C. H. Cheng, J. R. Williams, R. Macdonald, J. Knapczyk, M. Carman and A. Lopusinski, *J. Org. Chem.* **1983**, *48*, 661-665.